

University of Groningen

The application of fine TiO₂ particles for enhanced gas absorption

Dagaonkar, M.V.; Heeres, H.J.; Beenackers, A.A C M; Pangarkar, V.G.

Published in:
Chemical Engineering Journal

DOI:
[10.1016/S1385-8947\(02\)00188-2](https://doi.org/10.1016/S1385-8947(02)00188-2)

IMPORTANT NOTE: You are advised to consult the publisher's version (publisher's PDF) if you wish to cite from it. Please check the document version below.

Document Version
Publisher's PDF, also known as Version of record

Publication date:
2003

[Link to publication in University of Groningen/UMCG research database](#)

Citation for published version (APA):

Dagaonkar, M. V., Heeres, H. J., Beenackers, A. A. C. M., & Pangarkar, V. G. (2003). The application of fine TiO₂ particles for enhanced gas absorption. *Chemical Engineering Journal*, 92(1-3), 151 - 159. [PII S1385-8947(02)00188-2]. [https://doi.org/10.1016/S1385-8947\(02\)00188-2](https://doi.org/10.1016/S1385-8947(02)00188-2)

Copyright

Other than for strictly personal use, it is not permitted to download or to forward/distribute the text or part of it without the consent of the author(s) and/or copyright holder(s), unless the work is under an open content license (like Creative Commons).

The publication may also be distributed here under the terms of Article 25fa of the Dutch Copyright Act, indicated by the "Taverne" license. More information can be found on the University of Groningen website: <https://www.rug.nl/library/open-access/self-archiving-pure/taverne-amendment>.

Take-down policy

If you believe that this document breaches copyright please contact us providing details, and we will remove access to the work immediately and investigate your claim.

Downloaded from the University of Groningen/UMCG research database (Pure): <http://www.rug.nl/research/portal>. For technical reasons the number of authors shown on this cover page is limited to 10 maximum.

The application of fine TiO₂ particles for enhanced gas absorption

M.V. Dagaonkar^a, H.J. Heeres^{a,*}, A.A.C.M. Beenackers^{a,1}, V.G. Pangarkar^b

^a Department of Chemical Engineering, University of Groningen, Nijenborgh 4, 9747 AG Groningen, The Netherlands

^b Department of Chemical Engineering, University of Mumbai, Matunga, Mumbai 400 019, India

Accepted 6 July 2002

Abstract

The physical absorption of pure CO₂ in various liquids (water, hexadecane, and sunflower oil) containing micron sized TiO₂ particles has been investigated. Absorption studies were carried out in a batch stirred cell reactor at 298 K and initial pressures of 0.08 MPa. Solid loading and stirring intensities were varied systematically between 0–15 kg/m³ and 3.3–12.5 s^{−1}, respectively. Gas absorption rates are enhanced significantly in the presence of TiO₂ particles. Enhancement factors are a function of the solids loading and stirring intensity. Maximum enhancement factors of about 2 were observed for all solvents at low stirring intensities. The rate of gas absorption was theoretically analyzed using a heterogeneous unsteady state mass transfer model based on the Danckwerts surface renewal theory and a Langmuir-type of particle to interface adhesion isotherm. This model not only predicts the trends in the observed enhancement factors very well but also gives an accurate quantitative picture.

© 2002 Elsevier Science B.V. All rights reserved.

Keywords: Enhanced gas absorption; TiO₂ particles; Stirred cell reactor; Surface renewal model; Particle to interface adhesion isotherm

1. Introduction

The rate of gas absorption in a G–L or G–L–S contactor may be enhanced considerably by the presence of particles in the liquid-phase. To be effective, the particles have to be considerably smaller than the gas–liquid film thickness and need to have a high affinity for the component to be transferred [1–8]. Enhancement of the gas absorption rates due to the presence of small particles is explained by the so-called grazing or shuttle mechanism. It is assumed that the particles travel between the stagnant liquid mass transfer layer and the bulk of the liquid. Near the interface, the adsorptive particles are loaded with solute and the solute concentration in the liquid mass transfer layer will be reduced. As a consequence, the concentration gradient of the solute in the mass transfer layer will be increased, leading to enhanced gas absorption. After spending a certain time in the liquid side mass transfer layer, the particles returns to the bulk of the liquid where the gas-phase component is desorbed and the particle regenerated [1–8].

A large number of experimental studies have been performed on the (physical) absorption of various gases in aqueous activated carbon slurries. The absorption rates

increase with the activated carbon concentration until a certain concentration and then level off to a constant value [1–10]. Several explanations have been put forward to explain these effects. It is now widely accepted that, due to the hydrophobic properties of active carbon, the concentration of particles in the mass transfer zone is much higher than in the bulk of the suspension, leading to higher local absorption rates and higher enhancement factors [5,7,11,12].

Here, we describe our studies on the application of micron sized TiO₂ particles to enhance the absorption rates of CO₂ in various liquids. TiO₂ particles are potentially interesting to apply for enhanced gas absorption. Studies indicate that TiO₂ particles have a high adsorption affinity for certain gases (e.g. H₂, CO, CO₂, NH₃, etc.) [13,14]. Although the affinity may change dramatically in the presence of a liquid-phase, it certainly warrants further investigations. In addition, TiO₂ particles are relatively cheap and various grades are available with a broad spread in particle dimensions and distributions.

Enhancements in the gas absorption rates are expected to be a function of the hydrophobicity/hydrophilicity of the particles and as such are expected to be solvent depending. To study these effects for TiO₂ particles, the absorption experiments were carried out in three different solvents with a large spread in physical properties: water, hexadecane and sunflower oil.

* Corresponding author. Tel.: +31-50-363-4174; fax: +31-50-363-4479.
E-mail address: h.j.heeres@chem.rug.nl (H.J. Heeres).

¹ Deceased on 19 April 2001.

Nomenclature

a	gas–liquid interfacial area (m^2/m^3)
C_b	mass of gas absorbing particles per unit volume of bulk of the suspension (kg/m^3)
C_g	concentration of CO_2 in the gas-phase (mol/m^3)
C_L	concentration of CO_2 in the liquid-phase (mol/m^3)
C_A^*	concentration of component A in the liquid-phase at the gas–liquid interface (mol/m^3)
d_p	particle diameter (m)
D_A	solute diffusivity in the liquid-phase (m^2/s)
E	enhancement factor (–)
H	Henry number defined as $(C_A^*/C_g)_{\text{equilibrium}}$ (–)
He	Henry's constant ($\text{Pa m}^3/\text{mol}$)
J_A	mass transfer rate for the component A ($\text{mol}/\text{m}^2 \text{ s}$)
k	constant as defined in Eq. (4) (–)
k_a	particle adhesion coefficient (m^3/kg)
k_L	liquid side mass transfer coefficient (m/s)
k_{LS}	liquid side mass transfer coefficient of the covered part of the gas–liquid interface (m/s)
K_L	dimensionless liquid side mass transfer coefficient (–)
m	partition coefficient of the solute between the solid and the gas-phase (–)
p_A	partial pressure of the solute gas (Pa)
R	gas constant ($\text{J}/\text{mol K}$)
t	time (s)
T	temperature (K)
V_G	gas volume (m^3)
V_L	liquid volume (m^3)

Greek symbols

ζ	fraction of the gas–liquid interface covered by the adhering solid particles (–)
ζ_{max}	constant, as defined in Eq. (12) (–)
ρ_{PG}	density of the solid particle (kg/m^3)
σ	amount of carbon dioxide absorbed per unit mass of dry particles (mol/kg)

Superscripts

H_2O	water
0	value at time $t = 0$
∞	value at time $t = \infty$

2. Experimental

2.1. Reactor

The experiments were carried out in a thermostatic reactor of glass and stainless steel shown in Fig. 1. A six

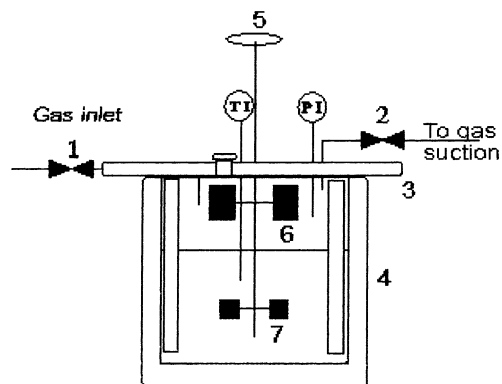


Fig. 1. Stirred cell reactor (1, 2: computer activated valves, 3: thermostated stainless steel top, 4: thermostated glass reactor wall, 5: medimix magnetic coupling, 6: gas stirrer, 7: liquid stirrer).

Table 1

Reactor dimensions

Reactor diameter	0.105 m
Reactor volume	$1.777 \times 10^{-3} \text{ m}^3$
Gas–liquid contact area	$8.37 \times 10^{-3} \text{ m}^2$
Liquid impeller type	Six bladed turbine, 0.04 m diameter
Gas impeller type	Six bladed turbine, 0.06 m diameter with enlarged blades

bladed Rushton turbine stirrer was located centrally in the liquid at a height above the reactor bottom equal to half the reactor diameter. Four symmetrically mounted glass baffles increased the effectiveness of stirring and prevented the formation of a vortex. The pressure and temperature transducers together with valves 1 and 2 were connected to an Olivetti M240 computer, enabling automatic data collection and programmed reactor operation. The reactor dimensions are given in Table 1.

2.2. Chemicals

The TiO_2 particles were obtained from Degussa, Germany. The average particle size was determined with a Coulter Counter Multisizer II and found to be $3 \mu\text{m}$. Hexadecane was purchased from Acros Organics, The Netherlands. The sunflower oil was a refined grade obtained from Unilever, Vlaardingen, The Netherlands. CO_2 (purity > 99.5%) was purchased from AGA GAS B.V., The Netherlands.

Table 2

Experimental data

Temperature	298 K
Initial pressure	$0.8 \times 10^5 \text{ Pa}$
Volume of slurry	$1 \times 10^{-3} \text{ m}^3$
Gas	CO_2 , purity > 99.5%
Stirrer speed	$3\text{--}13 \text{ s}^{-1}$
Average particle diameter (d_p)	$3 \mu\text{m}$
Density of the particles (ρ_{pg})	$3900 \text{ kg}/\text{m}^3$

2.3. Experiments

All the experiments were carried out batchwise, both with respect to gas-phase and the slurry solution. The slurry volume was $1 \times 10^{-3} \text{ m}^3$ and the slurry concentration varied between 0 and 15 kg/m^3 . The operating conditions are listed in Table 2.

In a typical experiment, the reactor was filled with the slurry (TiO_2 in distilled water, hexadecane or sunflower oil). The liquid was degassed by closing valve 1 and opening valve 2. Once the slurry was equilibrated under the vapor pressure of water, valve 2 was closed and CO_2 was fed to the reactor up to a fixed pressure (0.08 MPa). After closing valve 1, the stirrer was started and the decrease of pressure due to the physical absorption of CO_2 was recorded over time.

$$E = \left(\frac{\text{gas absorption flux in the suspension}}{\text{gas absorption flux in a particle free liquid}} \right)_{\text{similar hydrodynamic conditions}} \quad (8)$$

The interfacial area at higher speeds ($N > 6.5 \text{ s}^{-1}$) where the gas–liquid interface is no longer flat, was obtained by the procedure reported by Mehta and Sharma [15]. The interfacial area was found to remain unaffected in the speed range of $3\text{--}15 \text{ s}^{-1}$.

3. Data analysis, gas solubility and enhancement factors

The solubility of gas A in a liquid defined by Henry's law, is expressed by

$$He = \frac{p_A}{C_A^*} \text{ at equilibrium} \quad (1)$$

In the absence of chemical reaction, the Henry coefficient may be calculated from the experimental data using the following equation:

$$He = \frac{p^\infty - p^{\text{H}_2\text{O}}}{p^0 - p^\infty} \frac{RTV_L}{V_G} \quad (2)$$

The experimental value of the Henry coefficient for CO_2 in water was found to be close to the value provided in the literature ($3330 \text{ Pa m}^3/\text{mol}$). The values for CO_2 in hexadecane and sunflower oil were determined experimentally and were 3800 and $6600 \text{ Pa m}^3/\text{mol}$, respectively. These values are the average of at least three independent experiments.

Volumetric mass transfer coefficients were obtained from the physical absorption rate with time using the following equation:

$$\frac{k}{k+1} \ln \left(\frac{p_A^0}{(k+1)p_A - kp_A^0} \right) = k_L a t \quad (3)$$

where

$$k = \frac{V_G He}{V_L RT} \quad (4)$$

Eq. (3) is obtained from a mass balance for carbon dioxide for the gas-phase:

$$\frac{d(n_a)}{dt} = \frac{V_G}{RT} \frac{d(p_A)}{dt} = -J_A A = -k_L A \left(\frac{p_A}{He} - C_L \right) \quad (5)$$

The concentration of A in the liquid-phase (C_L) is eliminated by setting up a total mole balance for component A leading to

$$C_L = \frac{V_G}{RTV_L} [p_{A,0} - p_A] \quad (6)$$

Combination of Eqs. (5) and (6) leads to Eq. (3).

The rate of CO_2 absorption in the slurry follows from

$$J_A a = \frac{V_G}{V_L RT} \left(\frac{-dp_A}{dt} \right) \quad (7)$$

The experimental enhancement factor was calculated from

For various model calculations, e.g. the theoretical enhancement factors, the diffusion coefficients of CO_2 in the various liquids are required. The value for CO_2 in water is reported to be $1.95 \times 10^{-9} \text{ m}^2/\text{s}$ and for hexadecane $2.8 \times 10^{-9} \text{ m}^2/\text{s}$ [16]. The diffusion coefficient of CO_2 in the sunflower oil applied in our experimental studies was calculated using the Wilke–Chang equation and estimated to be $8 \times 10^{-11} \text{ m}^2/\text{s}$.

The partitioning coefficient of CO_2 between the solid and liquid-phase (m) is an important property of the system and was determined experimentally using the following relation:

$$\begin{aligned} m &= \frac{\text{amount of carbon dioxide per unit volume of particle}}{\text{amount of carbon dioxide per unit volume of liquid}} \\ &= \frac{\sigma \rho_{PG}}{C_G H} \end{aligned} \quad (9)$$

where σ is the amount of gas absorbed by the particle per unit mass of dry catalyst particle. This value is determined experimentally by taking the difference in the moles absorbed in a slurry and the moles absorbed in pure solvent devoid of adsorptive particles. The experimental values range between 310 for sunflower oil and 630 for water. For hexadecane, an intermediate value of 580 was obtained.

4. Theory

Various stationary and instationary models have been developed to describe the effects of particles on gas absorption rates [3,5,7,9,17–25]. The early stationary film theory models developed in the eighties of the previous century were later shown to be the special cases of a general, unsteady state theory developed by Mehra [26]. A recent overview dealing with these theoretical aspects has been provided by Beenackers and van Swaaij [8].

Wimmers and Fortuin [20,21] developed the first models, which take into account a non-uniform distribution of the

particles. Later, Vinke [7] presented an enhanced gas absorption model (EGAM) based on their work on absorption of H_2 in the aqueous suspensions containing different concentrations of small carbon-supported or alumina-supported catalyst particles. The model is based on the film theory of mass transfer combined with a particle to interface adhesion isotherm to take into account a non-uniform distribution of the particles in the liquid-phase.

Recently, Demmink et al. [12] formulated an unsteady state version of the EGAM model based on the surface renewal theory combined with particle to interface adhesion (SRPIA, surface renewal particle to interface adhesion model). This model has been applied to interpret the results obtained for acetylene absorption into aqueous solutions of iron chelates containing fine sulfur particles. This unsteady state model overcomes one of the basic limitations of the steady state, film theory based EGAM model, i.e. the inability to account for transient effects like solute accumulation in the particles. For initial enhancement (i.e. enhancement when the bulk solute concentration is zero), the following expression for the theoretical enhancement factor was derived:

$$E_{th} = \frac{J_A}{k_L C_A^*} = 1 + \zeta \times \left[\frac{1 - \tanh[K_L/4]}{3/(mK_L) + [1 + (3/mK_L)] \tanh[K_L/4]} \right] \quad (10)$$

where ζ is the surface fraction covered by particle and K_L a dimensionless mass transfer coefficient defined as

$$K_L = \frac{k_L d_p}{D_A} \quad (11)$$

where k_L is the mass transfer coefficient, D_A the diffusion coefficient of the solute in the liquid-phase and d_p the (average) particle size. ζ is the surface fraction covered by particles. The relationship between ζ and the particle concentration C_b in the liquid bulk is represented by a Langmuir-type adhesion isotherm:

$$\frac{\zeta}{\zeta_{max}} = \frac{k_a C_b}{1 + k_a C_b} \quad (12)$$

where k_a is the particle-to-gas interface adhesion constant and ζ_{max} the maximum fractional coverage of the G–L interface. ζ_{max} is a measure for the surface capacity of the particles and k_a a measure for the exchange equilibrium from particles moving to and away from the interface. Both parameters are a function of the speed of agitation. The values of ζ , k_a and ζ_{max} are determined from the individual absorption experiments using a procedure given by Vinke et al. [7]. The calculated values for k_a and ζ_{max} for the various experiments are given in Table 4.

According to the SRPIA model, the enhancement factor is a function of m , ζ and K_L (see Eq. (10)). When varying the value of K_L at constant values of m and ζ , the model predicts a maximum in the enhancement factor. The position and actual value of this maximum is a function of the values of m

and ζ [12]. This implies the occurrence of two different mass transfer regimes: one for which the enhancement increases with an increase in K_L (capacity controlled regime) and one for which the enhancement decreases with increasing K_L values (transport-controlled regime).

In the transport-controlled regime, the effect of particles on the gas absorption rate is determined solely by the rate at which the particles adsorb the solute. This situation occurs when the capacity of the particles is very high, i.e. the particle may be regarded as an infinite sink. When the gas absorption process occurs in the transport-controlled regime, higher stirring intensities will lead to lower enhancement factors. This is due to the fact that at higher intensities (i.e. high K_L values), the contact time of the particles at the G–L interface decreases and as a result, the particles leave the interface with less solute adsorbed, resulting in lower absorption rates.

The other extreme is called the solubility controlled or capacity controlled regime. Here, the absorption rate depends solely on the ultimate capacity of the particles and not on the rate of transport of solute to the particles. An increase in the stirring intensity and thus the frequency at which the particles are refreshed at the G–L interface will result in higher overall absorption rates and enhancement factors. The mass transfer rates of solute from the liquid-phase to the particles are not important in this regime and the particles are always fully saturated with solute.

Criteria to determine the regime for the absorption process have been derived for the SRPIA model. The transport-controlled regime holds when $K_L^2 m \gg 12$. For the capacity controlled regime, $\tanh((K_L/4)/(3/mK_L))$ should be $\ll 1$ and $mK_L \gg 3$.

5. Results and discussion

5.1. Absorption of CO_2 in aqueous TiO_2 slurries

Experiments were performed at different solid concentrations in the range of 0–1 kg/m³ and at speeds of agitation ranging from 3.3 to 9.2 s^{−1}. The observed experimental enhancement factors as a function of the solid loading are presented in Fig. 2. The results clearly indicate that the enhancement factors are depending on both the solids loading and the stirrer speed. The highest enhancement factor for this system was observed at the lowest stirring intensity (3.3 s^{−1}) and found to be 2.0 for a solid loading of 1 kg/m³.

The enhancement factors increase with an increase in the solid loading, however, appear to level off and ultimately reach a constant value at higher solids loading. The minimum solids concentration for maximum enhancement is about 0.5–0.7 kg/m³ for the experiments at a stirring intensity of 3.3 s^{−1}. This value is at the low end for the reported minimum solids concentration for various gas absorption studies in aqueous slurries containing small particles (0.2–10 kg/m³, see Table 3). The enhancement-loading

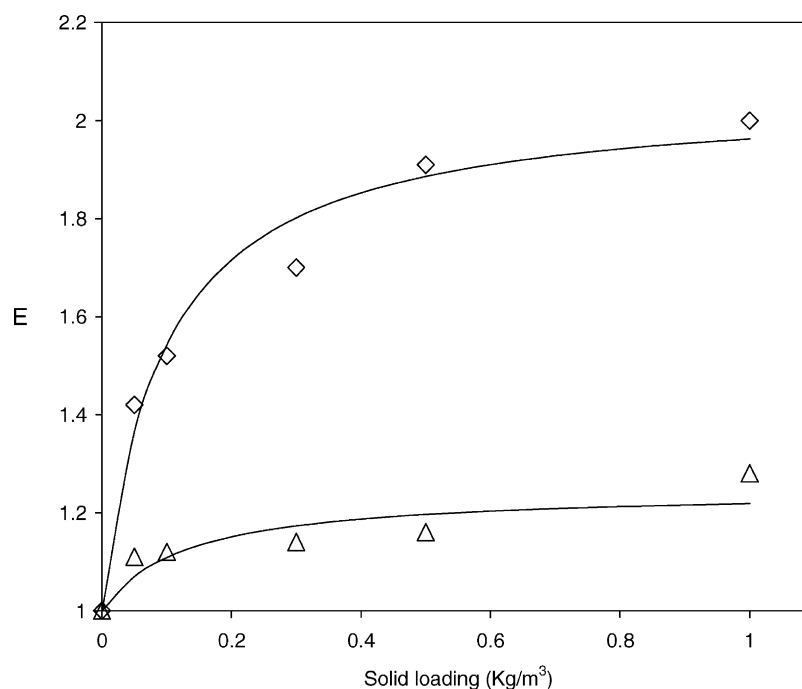


Fig. 2. Experimental enhancement factors as a function of solid loading at different stirrer speeds for the system $\text{TiO}_2/\text{water}$ (\diamond : 3.3 s^{-1} ; \triangle : 9.2 s^{-1}). The solid lines represent theoretical curves for enhancement factor calculated using Eq. (10) and the best-fit values of k_a and ζ_{\max} (Table 4).

profiles, i.e. a leveling off of the enhancement factors at high loading are typical for hydrophobic particles with a high affinity for the G–L interface [1–7,9,10].

The enhancement factor was found to decrease with an increase in the speed of agitation. This is evident when comparing the two extremes at a solid loading of 1 kg/m^3 (Fig. 2). The enhancement factor at low stirring intensity (3.3 s^{-1}) is nearly twice as high as for the highest speed of agitation (9.2 s^{-1}).

All observations, i.e. a leveling off of the enhancement factors at high solids loading and the effects of stirring speed are in accordance with the SRPIA model predictions. The leveling off at a high solids loading towards a constant enhancement value is the result of the fact that the surface fraction covered by particles (ζ) reaches a maximum value (ζ_{\max}). A further increase in the particle loading does not lead to higher concentration of particles near the G–L interface and beneficial effects on the absorption rates of CO_2

Table 3
Reported values for the solid loading for maximum enhancement

Serial number	System	$C_{s,\min}^a$ (kg/m^3)	d_p (μm)	Speed (s^{-1})	E^b
1	$\text{O}_2/(\text{glucose}/\text{Pt} + \text{ac. carbon})$ [1]	1	≤ 5	1–9	3.4
2	$\text{CO}_2/\text{ac. Carbon}$ [1]	2–3	≤ 5	2.9–7.8	3.92–2.28
3	$\text{Propane}/\text{ac. Carbon}$ [3]	–	34	–	–
4	$\text{CO}_2/(\text{Na}_2\text{CO}_3 + \text{ac. carbon})$ [1]	2–3	≤ 5	3	–
5	$\text{O}_2/(\text{Na}_2\text{SO}_3 + \text{ac. carbon})$ [17,27]	1	≤ 5	2	–
6	$\text{O}_2/(\text{Na}_2\text{S} + \text{ac. carbon})$ [1,4,10]	1 0.6–1.6	≤ 5 $\ll 10$ $\ll 100$	–	1.7
7	$\text{O}_2/(\text{aq. Glucose}/\text{Pt} + \text{ac. carbon})$ [9,11]	0.4 10	≤ 5 ≤ 5	2	3.2
8	$\text{CO}_2/(\text{aq. Na}_2\text{SO}_3 \text{ buffer}/\text{Pt} + \text{ac. carbon})$ [9,10,17,28]	2–3	≤ 20	1.5	–
9	$\text{CO}_2/(\text{alkanol amines} + \text{ac. carbon})$ [29]	6	$40\% < 1$	3	2
10	$\text{H}_2/\text{ac. carbon}$ [25]	0.6	10	3	3.3
	$\text{Ethene}/\text{ac. carbon}$ [25]	1.2	10	3	3.6
	$\text{Propane}/\text{ac. carbon}$ [25]	1.2	10	1.4	2
11	$\text{CO}_2/\text{ac. carbon}$ [30]	0.2	4–10	–	–
12	$\text{H}_2/(\text{H}_3\text{PO}_4 + \text{NH}_4\text{NO}_3 + \text{ac. carbon})$ [31]	1.5	40	13–30	3.6

^a $C_{s,\min}$: minimum solids loading for maximum enhancement.

^b E : enhancement factor as defined in Eq. (8).

Table 4

Calculated values for the values of Langmuir adhesion constants k_a and ζ_{\max} ^a

System		Stirrer speed (s^{-1})		
		3.3	7.5	9.2
TiO ₂ /water	ζ_{\max}	0.1 (0.01)	0.04 (0.01)	0.018 (0.004)
	k_a	10.6 (2.8)	5.9 (2.6)	7.9 (5.6)
TiO ₂ /hexadecane	ζ_{\max}	0.13 (0.01)	0.08 (0.003)	0.06 (0.004)
	k_a	1.3 (0.3)	1.3 (0.3)	0.7 (0.2)
TiO ₂ /sunflower oil	ζ_{\max}	0.34 (0.04)	0.15 (0.002)	–
	k_a	0.28 (0.08)	0.43 (0.1)	–

^a Values in parentheses are the standard deviation in the values calculated using standard statistical methods.

in the liquid-phase are not expected. The values of ζ_{\max} at different stirring intensities are given in Table 4 and were calculated to be 0.1 at $3.3 s^{-1}$ and 0.018 at $9.2 s^{-1}$.

The enhancement factors drop dramatically at higher stirring intensities (at similar solid loading, see Fig. 2). This may be explained by taking into account both (a) the fraction of the interface covered with particles and (b) the contact time of the particles at the G–L interface. Both factors are affected by the stirring intensity and will be discussed in the following.

The effective number of particles available for gas adsorption, i.e. the fractional coverage of the interface by the adsorbing particles (ζ), reduces with an increase in the speed of rotation. This is clearly expressed by the values of k_a and ζ_{\max} for the various stirring intensities (Table 4). Consequently, the gas absorption rates will be lowered at higher stirring intensities. Similar effects of stirring intensities on enhanced gas absorption were reported by Vinke et al. [7] for hydrogen absorption in aqueous active carbon slurries and Demmink et al. [12] for acetylene absorption in aqueous slurries containing sulfur particles.

Besides affecting the surface coverage, the stirring intensity also has an effect on the (dimensionless) mass transfer coefficient K_L . At higher stirring intensities, the mass transfer coefficient increases and according to the surface renewal theory, the contact time of the particles at the G–L interface reduces. Whether this has a positive or negative effect on the enhancement factors depends on the regime of mass transfer.

Application of the SRPIA and EGAM criteria suggest that the absorption process of CO₂ in aqueous TiO₂ slurries is transport-controlled at high stirrer speeds ($K_L^2 m > 20$). Hence, an increase in the stirring intensity (and an accompanying increase in the value of the dimensionless mass transfer coefficient K_L) will result in a lowering of the enhancement factor. Thus, it may be concluded that the observed drop in enhancement factors at higher stirring intensities (at similar solid loading, see Fig. 2) is due to a reduction in the surface fraction covered by particles and an increase in the dimensionless mass transfer coefficient K_L .

The experimental data were modeled using the SRPIA model (Table 5). The results for stirrer speeds of 3.3 and

Table 5

CO₂ absorption data for TiO₂–water slurries

Stirrer speed (s^{-1})	Solid loading (kg/m^3)	$E_{\text{experimental}}$	$E_{\text{theoretical}}^a$
3.3	0.05	1.42	1.36
	0.1	1.52	1.54
	0.3	1.70	1.80
	0.5	1.91	1.88
	1	2.0	1.96
7.5	0.05	1.04	1.11
	0.1	1.23	1.18
	0.3	1.35	1.30
	0.5	1.40	1.36
	1	1.41	1.41
9.2	0.05	1.11	1.07
	0.1	1.12	1.11
	0.3	1.14	1.17
	0.5	1.16	1.19
	1	1.28	1.22

^a Theoretical enhancement factor according to SRPIA model (Eq. (10)).

$9.2 s^{-1}$ are presented in Fig. 2. It is evident that the observed trends for the enhancement factors as a function of the loading (leveling off at higher loading) as well as stirrer speed (lower enhancement at higher stirring intensities) are described properly by the model.

5.2. Absorption of CO₂ in hexadecane

Experiments were performed at different TiO₂ concentrations in the range of 0–10 kg/m^3 and at speeds of agitation ranging from 3.3 to 12.5 s^{-1} . The experimental enhancement factors as a function of the solid loading are presented in Fig. 3 for the extremes of the stirrer speeds (3.3 and 12.5 s^{-1} , see also Table 6). The highest enhancement factor for this system was found to be 1.9 for a solid loading of 10 kg/m^3 at a stirrer speed of 3.3 s^{-1} .

Analogous to the TiO₂/water systems, the enhancement factors level off at higher solids loading. Beyond a solid loading of about 4–6 kg/m^3 , there is no significant enhancement in the rate of gas absorption. This is the minimum solid loading for maximum enhancement and is an order of magnitude higher than that found for the TiO₂/water system (0.5–0.7 kg/m^3).

It is interesting to compare the experimental enhancement factors at similar solid loading for the TiO₂/water and TiO₂/hexadecane system. The enhancement factors for hexadecane are lower than for water, especially at the low stirring intensities. For instance, at 3.3 s^{-1} and a loading of 1 kg/m^3 , the enhancement factors are 1.57 for hexadecane and 2.0 for water. According to the SRPIA model, enhancement factors are a function of the surface coverage ζ , the dimensionless mass transfer coefficient K_L and the solute partition coefficient m (see Eq. (10)).

The values for the partitioning coefficient m do not differ dramatically (630 for water and 580 for hexadecane).

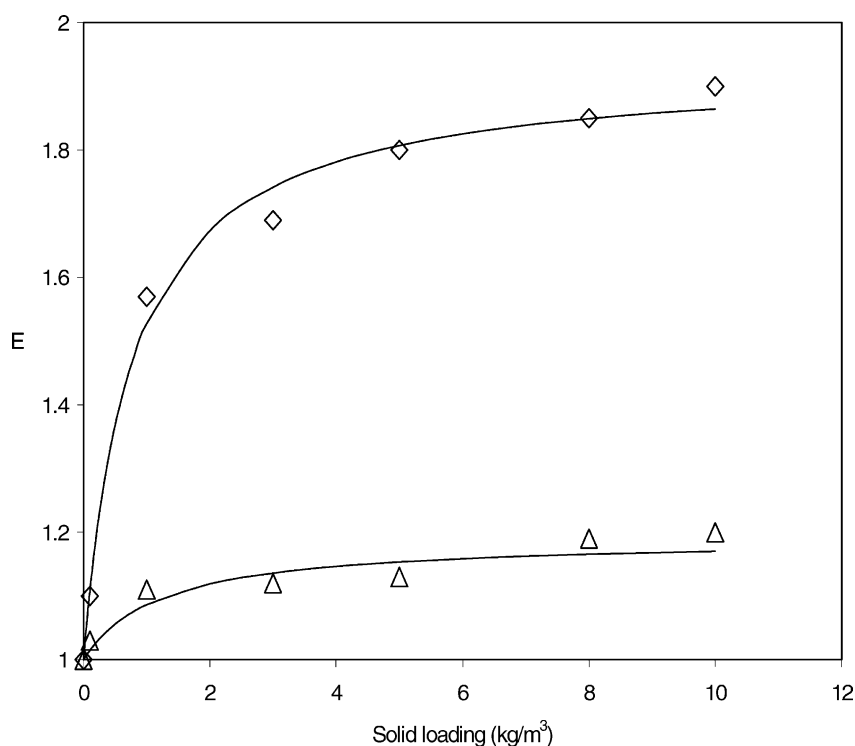


Fig. 3. Experimental enhancement factors as a function of solid loading at different stirrer speeds for the system TiO_2 /hexadecane (\diamond : 3.3 s^{-1} ; \triangle : 12.5 s^{-1}). The solid lines represent theoretical curves for enhancement factor calculated using Eq. (10) and the best-fit values of k_a and ζ_{\max} (Table 4).

Differences are found for both the value of the dimensionless mass transfer coefficient K_L and the surface coverage ζ . The K_L values for water are slightly higher than for hexadecane, mainly due to the differences in the diffusivity of carbon dioxide in both media. The fractional coverage

of the surface with particles under similar hydrodynamic conditions differs significantly for both solvents. This is clearly expressed by the value of the particle to gas interface adhesion constant k_a (Table 4). The k_a values in water are significantly higher than for hexadecane. This implies that the titanium dioxide particles in water have a higher affinity for the G–L interface than in an apolar solvent like hexadecane. It suggests that titanium dioxide particles may be considered as rather hydrophobic. Additional information to support this conclusion may be obtained from contact angle measurements. When a liquid is placed on a solid, the liquid in most cases remains as a drop on the surface with a definite angle of contact between the liquid and solid-phase [32]. This contact angle is a measure for wetting tendency of a liquid. Small contact angles are indicative for a good wetting ability and adhesion between the liquid and solid-phase. Contact angle measurements for a number of solvents in combination with TiO_2 have been reported [33]. Contact angles for water are higher than for typical organic solvents, indicating that titanium dioxide is indeed hydrophobic in nature.

Application of the SRPIA model to determine the absorption regime suggest that the absorption of CO_2 in TiO_2 /hexadecane takes place in an intermediate regime, i.e. is neither capacity controlled nor transport-controlled. The solid curves in Fig. 3 are the theoretical enhancement factors calculated using the SRPIA model and the best-fit values of k_a and ζ_{\max} . Agreement between experimental data and model prediction is very satisfactory.

Table 6
 CO_2 absorption data for TiO_2 –hexadecane slurries

Stirrer speed (s^{-1})	Solid loading (kg/m^3)	$E_{\text{experimental}}$	$E_{\text{theoretical}}^a$
3.3	0.1	1.1	1.11
	1	1.57	1.53
	3	1.69	1.74
	5	1.80	1.81
	8	1.85	1.85
	10	1.90	1.86
7.5	0.1	1.1	1.08
	1	1.42	1.41
	3	1.56	1.56
	5	1.62	1.62
	8	1.68	1.65
	10	1.72	1.66
12.5	0.1	1.03	1.01
	1	1.11	1.09
	3	1.12	1.14
	5	1.13	1.15
	8	1.19	1.16
	10	1.23	1.18

^a Theoretical enhancement factor according to SRPIA model (Eq. (10)).

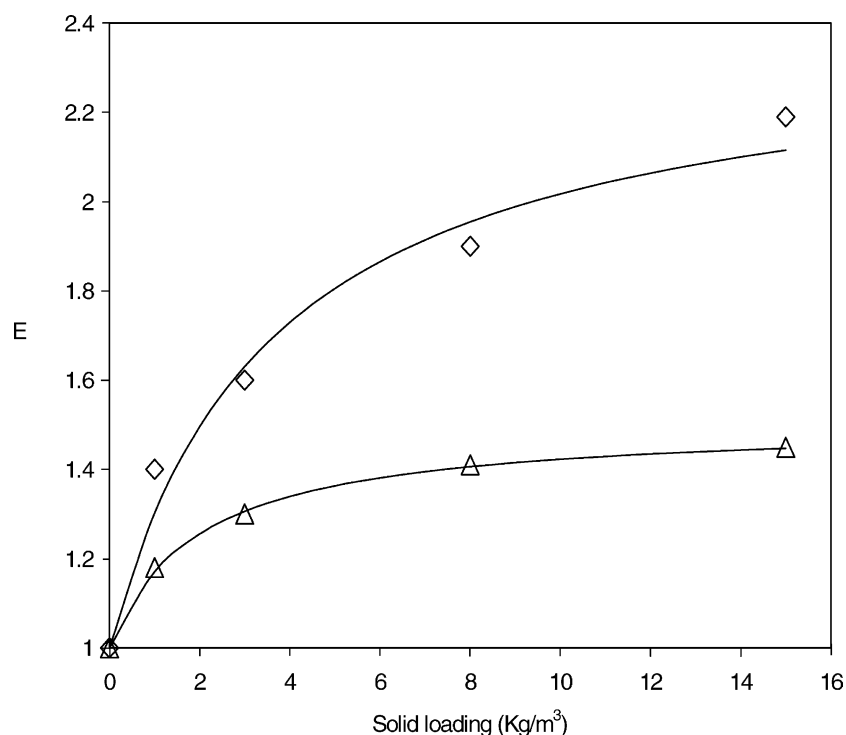


Fig. 4. Experimental enhancement factors as a function of solid loading at different stirrer speeds for the system TiO_2 /sunflower oil (\diamond : 3.3 s^{-1} ; \triangle : 7.5 s^{-1}). The solid lines represent theoretical curves for enhancement factor calculated using Eq. (10) and the best-fit values of k_a and ζ_{\max} (Table 4).

5.3. Absorption of CO_2 in sunflower oil

The results of the CO_2 absorption experiments in TiO_2 dispersed in sunflower oil are given in Table 7 and shown in Fig. 4 in the form of enhancement factors as a function of solid loading. The highest enhancement factor for this system was found to be 2.2 for $C_s = 15 \text{ kg/m}^3$ at 3.3 s^{-1} . The qualitative trends are again similar as for the TiO_2 /water and TiO_2 /hexadecane systems, i.e. a leveling off of the enhancement factor at higher particle loading and a lowering of the enhancement at higher stirring intensities. The major difference is the value of the minimum solids loading for maximum enhancement, which is significantly higher ($>5 \text{ kg/m}^3$) than for the other two systems. Hence, higher

solids loading are required for maximum enhancement in gas absorption rates.

Furthermore, the enhancement factors at a particular solid loading and stirring intensity for the TiO_2 –sunflower oil system are always lower than for the other two systems. This is the result of the large difference in viscosities of the liquids, resulting in a significant lower value of the diffusion coefficient of CO_2 in the relatively viscous sunflower oil. As a result, the values of the liquid side mass transfer coefficient (k_L) for CO_2 –sunflower oil are on average a factor of 2 lower than found for water.

The high viscosity of sunflower oil also has an impact on the absorption regime. The value of the parameter $K_L^2 m$ is the highest for all solvents studies (>100) and it is evident that CO_2 absorption takes place in the transport-controlled regime.

Table 7
 CO_2 absorption data for TiO_2 –sunflower oil slurries

Stirrer speed (s^{-1})	Solid loading (kg/m^3)	$E_{\text{experimental}}$	$E_{\text{theoretical}}^a$
3.3	1	1.4	1.30
	3	1.6	1.63
	8	1.9	1.95
	15	2.2	2.11
7.5	1	1.2	1.17
	3	1.3	1.30
	8	1.4	1.41
	15	1.45	1.45

^a Theoretical enhancement factor according to SRPIA model (Eq. (10)).

6. Conclusions

This research has demonstrated that micron sized TiO_2 particles are capable of enhancing the physical absorption rate of CO_2 in various liquids (water, hexadecane, and sunflower oil). The maximum enhancement factors were found to be about 2 for all solvents under study. Enhancement factors were a function of the solid loading and the stirring intensity. Upon increasing the solid loading, the enhancement factor increases and then levels off to a constant value. The minimum solid loading required for maximum enhancement

was depending on the nature of the liquid-phase and increased upon going from water ($0.5\text{--}0.7\text{ kg/m}^3$) to hexadecane ($4\text{--}6\text{ kg/m}^3$) and sunflower oil ($>5\text{ kg/m}^3$).

The experimental data were modeled using an unsteady state model based on the Danckwerts surface renewal theory using a particle to surface adhesion isotherm. This SRPIA model not only described the observed effects in a qualitative way but also the quantitative agreement was very satisfactory. This implies that the TiO_2 particles are non-uniformly distributed between the bulk liquid-phase and the liquid film-layer and have a high affinity to stick to the gas–liquid interface.

Based on this study, it may be concluded that micron sized TiO_2 particles may be attractive alternatives for active carbon materials to enhance mass transfer of gaseous components to a liquid-phase. Typical experimental problems encountered when using a natural product like active carbon, i.e. strong effects of pre-treatment procedures on the absorption results, may be overcome by using well-defined TiO_2 particles. Further experimental work in typical industrial contactors (e.g. bubble column reactors) will be required to fully assess the potential of these interesting micron sized TiO_2 particles for enhanced mass transfer rates.

References

- [1] K. Chandrasekaran, M.M. Sharma, Absorption of oxygen in aqueous solutions of sodium sulfide in the presence of activated carbon as catalyst, *Chem. Eng. Sci.* 32 (1977) 669.
- [2] G.E.H. Joosten, J.G.M. Schilder, J.J. Janssen, The influence of suspended solid material on the gas–liquid mass transfer in stirred gas–liquid contactors, *Chem. Eng. Sci.* 32 (1977) 563.
- [3] R.L. Kars, R.J. Best, A.A.H. Drinkenburg, The sorption of propane in slurries of active carbon in water, *Chem. Eng. J.* 17 (1979) 201.
- [4] S.K. Pal, M.M. Sharma, V.A. Juvekar, Fast reactions in slurry reactors: catalyst particle size smaller than film thickness: oxidation of aqueous sodium sulfide solutions with activated carbon particles as catalyst at elevated temperatures, *Chem. Eng. Sci.* 37 (1982) 327.
- [5] O.J. Wimmers, J.M.H. Fortuin, Determination of the enhancement factor for gas absorption in a slurry reactor, *Istn. Chem. Engrs. Symp. Ser.* 87 (1984) 195.
- [6] G. Quicker, E. Alper, W.D. Deckwer, Effect of fine activated carbon particles on the rate of CO_2 absorption, *AIChE J.* 33 (1987) 871.
- [7] H. Vinke, P.J. Hamersma, J.M.H. Fortuin, Enhancement of the gas-absorption rate in agitated slurry reactors by gas-adsorbing particles adhering to gas bubbles, *Chem. Eng. Sci.* 48 (1993) 2197.
- [8] A.A.C.M. Beenackers, W.P.M. van Swaaij, Mass transfer in gas–liquid slurry reactors, *Chem. Eng. Sci.* 48 (18) (1993) 3109.
- [9] E. Alper, B. Wichtendahl, W.D. Deckwer, Gas absorption mechanism in catalytic slurry reactors, *Chem. Eng. Sci.* 35 (1980) 217.
- [10] E. Alper, S. Ozturk, Effect of fine solid particles on gas–liquid mass transfer rate in a slurry reactor, *Chem. Eng. Commun.* 46 (1986) 147.
- [11] Y.Y. Lee, G.T. Tsao, Oxygen absorption into glucose solution, *Chem. Eng. Sci.* 27 (1972) 1601.
- [12] J.F. Demmink, Removal of hydrogen sulfide and nitric oxide with iron chelates, Ph.D. Thesis, University of Groningen, The Netherlands, 2000;
- [13] J.F. Demmink, A. Mehra, A.A.C.M. Beenackers, Gas absorption in the presence of particles showing interfacial affinity: case of fine sulfur precipitates, *Chem. Eng. Sci.* 53 (1998) 2885.
- [14] A.L. Linsebigler, L. Guangquan, Y.T. Yates, Photocatalysis on TiO_2 surfaces: principles, mechanisms and selected results, *Chem. Rev.* 95 (1995) 735.
- [15] K. Tanaka, J.M. White, Characterization of species adsorbed on oxidised and reduced anatase, *J. Phys. Chem.* 86 (1982) 4708.
- [16] V.D. Mehta, M.M. Sharma, Mass transfer in mechanically agitated gas–liquid contactors, *Chem. Eng. Sci.* 26 (1971) 461.
- [17] R.H. Perry, D. Green, *Perry's Chemical Engineers' Handbook*, 6th ed., McGraw-Hill, New York, 1984.
- [18] E. Alper, W.D. Deckwer, Some aspects of gas absorption mechanism in slurry reactors, NATO ASI Series E, No. 73, vol. 2, Martinus Nijhoff, The Hague, 1983.
- [19] O.J. Wimmers, R. Paulussen, D.P. Vermeulen, J.M.H. Fortuin, Enhancement of absorption of a gas into a stagnant liquid in which a heterogeneously catalysed chemical reaction occurs, *Chem. Eng. Sci.* 39 (1984) 1415.
- [20] R.D. Holstvoogd, K.J. Ptasiński, W.P.M. van Swaaij, Penetration model for gas absorption with reaction in slurry containing fine insoluble particles, *Chem. Eng. Sci.* 41 (1986) 867.
- [21] O.J. Wimmers, J.M.H. Fortuin, The use of adhesion of catalyst particles to gas bubbles to achieve enhancement of gas absorption in slurry reactors. I. Investigation of particle to bubble adhesion using the bubble pick-up method, *Chem. Eng. Sci.* 43 (1988) 303.
- [22] O.J. Wimmers, J.M.H. Fortuin, The use of adhesion of catalyst particles to gas bubbles to achieve enhancement of gas absorption in slurry reactors. II. Determination of the enhancement in a bubbles-containing slurry reactor, *Chem. Eng. Sci.* 43 (1988) 313.
- [23] R.D. Holstvoogd, W.P.M. van Swaaij, L.L. van Dierendonck, The adsorption of gases in aqueous activated carbon slurries enhanced by adsorbing or catalytic particles, *Chem. Eng. Sci.* 43 (1988) 2181.
- [24] S. Karve, V.A. Juvekar, Gas absorption into slurries containing fine catalyst particles, *Chem. Eng. Sci.* 45 (1990) 587.
- [25] R.D. Holstvoogd, W.P.M. van Swaaij, The influence of sorption capacity on enhanced gas absorption in activated carbon slurries, *Chem. Eng. Sci.* 45 (1990) 151.
- [26] J.T. Tinge, A.A.H. Drienkenburg, The enhancement of the physical absorption of gases in aqueous activated carbon slurries, *Chem. Eng. Sci.* 50 (1995) 937.
- [27] A. Mehra, Intensification of multiphase reactions through the use of microphase. I. Theoretical, *Chem. Eng. Sci.* 43 (1988) 899.
- [28] E. Alper, Kinetics of absorption of oxygen into aqueous solutions of sodium sulfide containing finely powdered activated carbon in a slurry reactor, *Chem. Eng. Commun.* 36 (1985) 45.
- [29] E. Sada, H. Kumazawa, Some considerations on chemical absorption into a slurry containing fine catalyst particles, *Chem. Eng. Sci.* 37 (1982) 945.
- [30] A.K. Saha, S.S. Bandhopadhyay, A.K. Biswas, Absorption of carbon dioxide in alkanol amines in the presence of fine activated carbon particles, *Can. J. Chem. Eng.* 70 (1992) 193.
- [31] G. Quicker, E. Alper, W.D. Deckwer, Gas absorption rates in a stirred cell with plane interface in the presence of fine particles, *Can. J. Chem. Eng.* 67 (1989) 32.
- [32] D. Lindner, M. Werner, A. Schumpe, Hydrogen transfer in slurries of carbon supported catalyst (HPO process), *AIChE J.* 34 (1988) 1691.
- [33] A.W. Adamson, *Physical Chemistry of Surfaces*, 5th ed., Wiley, New York, 1990.
- [34] R. Wang, K. Hashimoto, A. Fuijishima, M. Chikuni, E. Kojima, A. Kitamura, M. Shimohigoshi, T. Watanabe, Photogeneration of highly amphiphilic TiO_2 surfaces, *Adv. Mater.* 10 (1998) 135.